Article

Not peer-reviewed version

Entanglement Missed Detection of Two-Mode Squeezed States Based on Inseparability Criterion

Chunxiao Cai * , Wenting Diao * , Fupan Feng , Wenhai Yang , Xinyu Su , Weigang Zhao , Jinman Ge , Long Ma , Nan Huo , Yanhong Liu , Chongdi Duan

Posted Date: 31 October 2024

doi: 10.20944/preprints202410.2541.v1

Keywords: Gaussian quantum entanglement; inseparability criterion; entanglement asymmetry

Article

Entanglement Missed Detection of Two-Mode Squeezed States Based on Inseparability Criterion

Chunxiao Cai [1,*], Wenting Diao [1,*], Fupan Feng [1], Wenhai Yang [1], Xinyu Su [1], Weigang Zhao [1], Jinman Ge [1], Long Ma [2], Nan Huo [3], Yanhong Liu [4] and Chongdi Duan [1]

[1] National Key Laboratory of Science and Technology on Space Microwave, China Academy of Space Technology (Xi'an), Xi'an 710100, China
[2] School of Computer Science and Engineering, Chongqing Three Gorges University, Chongqing 404100, China
[3] Shanxi Center of Technology Innovation for Light Manipulations and Applications, School of Applied Science, Taiyuan University of Science and Technology, Taiyuan 030024, China
[4] Department of Physics, Taiyuan Normal University, Jinzhong 030619, China
* Correspondence: caicx1@cast504.com (C.C.); dwt1124@163.com (W.D.)

Abstract: The inseparability criterion provides a straightforward and efficient method for identifying and quantifying two-mode Gaussian quantum entanglement, making it a crucial tool in quantum optics experiments. However, it is crucial to recognize that the inseparability criterion serves only as a sufficient condition for entanglement assessment, thereby posing a risk of missed detection during evaluation. This paper investigates the use of the inseparability criterion in assessing two-mode squeezed states, with a particular focus on examining missed entanglement detection due to entanglement asymmetry. The results show that when decoherence symmetrically affects both modes, the inseparability criterion effectively detects entanglement. In contrast, when this symmetry is broken, the criterion may fail to identify entanglement, with the likelihood of missed detection increasing alongside rising asymmetry. By comparing these results with the positive partial transpose criterion, which serves as a necessary and sufficient condition, the occurrence of missed detections by the inseparability criterion is confirmed. Our research not only provide valuable insights into the application of the inseparability criterion in quantum information tasks but also deepens the understanding of its operational principles and limitations.

Keywords: Gaussian quantum entanglement; inseparability criterion; entanglement asymmetry

---

Introduction

Quantum entangled states are fundamental resources in quantum information physics, offering unparalleled advantages over classical resources in critical tasks such as information processing [1,2], communication [3–5], and computation [6]. Two-mode squeezed states [7], exemplars of continuous-variable entanglement, have attracted significant attention due to their pivotal roles in advancing quantum optics and quantum information technologies. Generated through nonlinear optical processes like optical parametric amplification or oscillation, these states exhibit remarkable squeezing effects in both joint amplitude and phase correlations of the two optical modes in phase space [8], reinforcing their indispensable status in quantum information science. Their significance extends to applications such as quantum illumination [9,10] and continuous-variable quantum key distribution [11,12].

The detection and assessment of quantum entanglement are central topics in quantum information theory, serving as essential prerequisites for the practical deployment of quantum technologies. In quantum communication, accurate entanglement evaluation directly impacts the security and efficiency of information transmission. Similarly, in quantum computation, precise entanglement measurement underpins the achievement of algorithmic acceleration and quantum parallelism. To this end, researchers have developed various entanglement criteria [13], including the Einstein-Podolsky-Rosen (EPR) paradox [14], the positive partial transposition (PPT) criterion [15], relative entanglement entropy [16], and the inseparability criterion [17]. These criteria determine whether a system is in an entangled or separable state by measuring the expectation values of specific observables. Among these, the inseparability criterion, renowned for its simplicity and experimental feasibility, has been extensively employed in quantum optics experiments. Introduced by Duan et al. [17] and Simon [15], the criterion relies on measuring the total variance of EPR-type operator pairs and comparing it with the standard quantum limit to ascertain entanglement. Researchers have leveraged this criterion to explore the dynamical behavior of entangled states in complex environments, such as noisy and lossy channels [18–21]. Notably, studies like those by D. Buono et al. have validated the robustness of entangled states under strong decoherence using various quantum indicators, including teleportation fidelity, quantum discord, mutual information, and the inseparability criterion [22]. W. P. Bowen et al. investigated the effects of symmetric decoherence on the EPR paradox and inseparability criterion, revealing their qualitative disparities [23]. Furthermore, the inseparability criterion has been extended to assess intricate multi-mode Gaussian quantum entangled states, such as four-mode cluster states [24] and hyperentangled states simultaneously possessing orbital angular momentum and spin angular momentum [25], highlighting its versatility. While previous research primarily focused on symmetric channel decoherence, the increasing importance of asymmetric decoherence phenomena in quantum communication and computation underscores the need for closer examination under asymmetric conditions. Genta Masada have addressed the challenges posed by asymmetric entanglement and channel losses in quantum illumination systems, utilizing the inseparability criterion to analyze the evolution of non-classical correlations [26–30]. Feng et al. [31] and Zhao Hao et al. [32] have also contributed to this field by characterizing the transmission evolution of entangled fields in optical fibers and analyzing the impact of state asymmetry on entanglement properties and robustness [31,32]. Research by WENHUI ZHANG et al. further reinforces this trend, emphasizing the significance of exploring quantum entanglement under asymmetric decoherence conditions [33].

The inseparability criterion stands as a sufficient condition for assessing entanglement, proficiently identifying its presence in diverse scenarios. Nevertheless, its non-necessity poses a limitation: in situations characterized by significant asymmetry within the system, particularly those involving asymmetric decoherence or intrinsic quantum state asymmetry, it may fall short of fully and precisely quantifying the extent of entanglement, thereby posing a risk of missed entanglement detections and ultimately leading to an underestimation of the entanglement degree. This limitation transcends specific applications like quantum illumination for target recognition and ranging [34,35], one-sided device-independent quantum key distribution [36], and correlated quadrature asymmetries in entanglement [37,38], posing a tangible threat to the operational integrity of quantum technologies. The complexities inherent in asymmetric quantum systems present a significant challenge to the inseparability criterion, impairing its capacity to fully capture the intricacies of entangled states. As a result, there exists a risk of underestimating the degree of entanglement and missing crucial detections, which could, in turn, jeopardize the practical implementation of quantum technologies. In quantum communication, missed detections may compromise the security of information transmission, while in quantum computation, they may threaten the accuracy of algorithm execution and the reliability of outcomes. Therefore, it is imperative to rigorously evaluate the strengths and limitations of the inseparability criterion in these contexts.

In this paper, we investigate the vulnerability of missed entanglement detections when applying the inseparability criterion to asymmetric two-mode squeezed states. We undertake a comparative analysis with the PPT criterion, known for its superior entanglement detection capabilities, theoretically and experimentally examining how entanglement mode asymmetry modulates the effectiveness of these criteria. Our methodology illuminates the mechanism behind undetected entanglement by the inseparability criterion. By artificially inducing controlled asymmetric optical losses in the distribution of two-mode squeezed states, we simulate experimental asymmetry. Our results reveal a nuanced picture: in symmetric settings, the inseparability criterion aligns with the PPT criterion, fulfilling both sufficiency and necessity for entanglement measurement. Conversely, in asymmetric environments, it reduces to a sufficient condition, incapable of fully and accurately capturing the extent of entanglement. This underscores the crucial importance of judiciously selecting entanglement criteria tailored to specific quantum information processing applications to ensure accurate and reliable entanglement detection. Our contribution aims to propel the advancement of

Preprints.org (www.preprints.org) | NOT PEER-REVIEWED | Posted: 31 October 2024 doi:10.20944/preprints202410.2541.v1

more efficient entanglement verification strategies, indispensable for the robust implementation of real-world quantum systems.

2. Theoretical Analysis

2.1. Asymmetry of Two-Mode Gaussian States

The two-mode squeezed state is a fundamental Gaussian quantum state in quantum optics, typically generated by a type-II nondegenerate optical parametric amplifier (NOPA) or by combining two independent single-mode squeezed fields using a 50/50 beam splitter. Mathematically, this state can be described by the symplectic eigenform of its covariance matrix, denoted as $\boldsymbol{\sigma}_{ij} = \langle (X_i X_j + X_j X_i) \rangle / 2 - \langle X_i \rangle - \langle X_j \rangle$, where $X \equiv \left(X_a^+, X_a^-, X_b^+, X_b^- \right)$ represents the quadrature components of the field. The quadrature amplitude operator X_i^+ and the quadrature phase operator X_i^- are defined in terms of the annihilation operator a_i and creation operator a_i^+ of the field as $X_i^+ = a_i + a_i^+$ and $X_i^- = i\left(a_i^+ - a_i\right)$,

$$\boldsymbol{\sigma} = \begin{bmatrix} \boldsymbol{A} & \boldsymbol{C} \\ \boldsymbol{C}^T & \boldsymbol{B} \end{bmatrix} = \begin{bmatrix} n & 0 & c_1 & 0 \\ 0 & n & 0 & c_2 \\ c_1 & 0 & m & 0 \\ 0 & c_2 & 0 & m \end{bmatrix} \tag{1}$$

where the submatrices $\boldsymbol{A}$ and $\boldsymbol{B}$ correspond to the autocovariance matrices of the two subsystems, while the off-diagonal elements $\boldsymbol{C}$ represent the cross-covariance matrix between the two subsystems [39]. The relevant quantities n, m, c_1 and c_2 are determined by four local symplectic invariants: $\det \boldsymbol{\sigma} = \left(nm - c_1^2\right)\left(nm - c_2^2\right)$, $\det \boldsymbol{A} = n^2$, $\det \boldsymbol{B} = m^2$ and $\det \boldsymbol{C} = c_1 c_2$. Notably, the parameters are not arbitrary but must subject to specific physical constraints [22]:

$$\boldsymbol{\sigma} + \frac{i}{2}\boldsymbol{\omega} \oplus \boldsymbol{\omega} \geq 0 \tag{2}$$

where $\boldsymbol{\omega} \equiv \begin{pmatrix} 0 & 1 \\ -1 & 0 \end{pmatrix}$. These constraints can be further elucidated as a function of the symplectic eigenvalues of the matrix elements, providing a deeper understanding of the state's properties,

$$\det \boldsymbol{A} + \det \boldsymbol{B} + 2\det \boldsymbol{C} \leq 4\det \boldsymbol{\sigma} + 1 \tag{3}$$

A state is termed symmetric when the covariance matrix satisfies $n = m$. For an ideal symmetric state, the parameters in the covariance matrix satisfy both $n = m$ and $c_1 = -c_2$

However, in practical applications, imperfections such as equipment noise and operational inefficiencies often result in asymmetry in two-mode squeezed states [40]. As illustrated in Figure 1, this asymmetry manifests primarily in two aspects: asymmetry in the orthogonal components of inter-mode correlations and asymmetry between the entangled modes. The former refers to the difference between the inter-mode covariance components c_1 and c_2. This asymmetry typically arises from inconsistencies in the degree of squeezing, squeezing direction, or phase differences between the two squeezed beams (SQ1 and SQ2) used to generate the two-mode squeezed state during the state preparation process [23]. Mode asymmetry, on the other hand, refers to the difference between the local covariance matrices n and m of the two modes. This asymmetry is often a result of the state transmission and detection processes, commonly encountered in quantum information protocols involving asymmetric noise and loss channels, such as quantum illumination and one-sided device-independent quantum key distribution. Asymmetry can significantly impact the results of entanglement criteria, making it crucial to understand and analyze the effects in practical systems.

 doi:10.20944/preprints202410.2541.v1

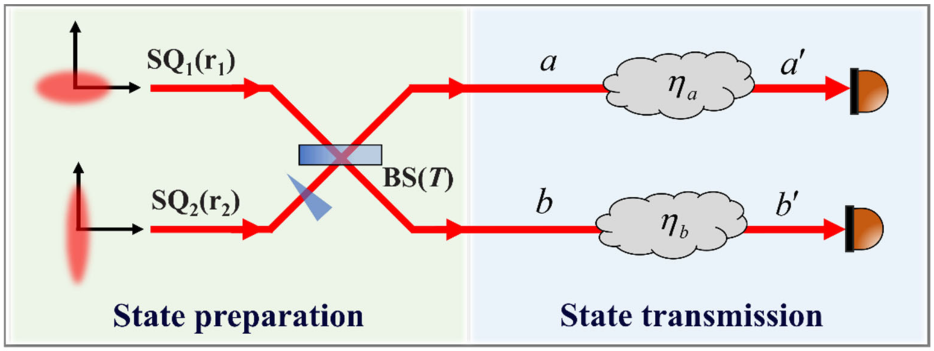

Figure 1. The diagram illustrates the asymmetry of a two-mode squeezed state, where the asymmetry of the associated orthogonal components and the asymmetry of the entanglement modes are significantly manifested in the preparation and transmission stages, respectively.

2.2. Missed Detection of Entanglement

The covariance matrix, as a vital representation of quantum state statistical information, provides a comprehensive statistical description of the correlation characteristics of two-mode squeezed states. However, it does not directly reveal the separability or entanglement of a state, nor does it quantify the degree of entanglement, necessitating the use of specific entanglement criteria. Inseparability criteria are widely employed in optical experiments, offering a straightforward and efficient tool for investigating the entanglement properties of continuous-variable quantum systems. The criteria typically equate separability with the positivity of the P-function. For states characterized by Gaussian noise distributions and symmetric correlations in conjugate quadrature components, the criteria can be linked to measurable correlations [6]. Specifically, for two-mode squeezed states, the inequality takes the form of:

$$Ent_{Inse} = \Delta^2 X^{+}_{a\pm b} + \Delta^2 X^{-}_{a\pm b} < 1 \tag{4}$$

where $\Delta^2 X^{+}_{a\pm b}$ represents the minimum value of the variance of the sum or difference of operators between beams a and b, which has been normalized, i.e., $\Delta^2 X^{+}_{a\pm b} = \min\left\langle \left(\delta X^{+}_{a} \pm \delta X^{+}_{b}\right)^2 \right\rangle / 4$. The elements of covariance matrix can be further utilized to calculate these variances:

$$Ent_{Inse} = \frac{1}{4}\left(\alpha + \beta \pm 2\gamma\right) < 1 \tag{5}$$

The value of Ent_{Inse} directly reflects the strength of entanglement in the quantum state. The closer the value is to zero, the higher the degree of entanglement. It is important to note that the inseparability criterion is merely a sufficient condition for entanglement. Specifically, satisfying this inequality confirms the existence of entanglement. However, this criterion is not necessary — satisfying inequality (4) does not guarantee that the state is separable. The inseparability criterion fails to capture all entangled states, meaning certain entangled states may not satisfy this criterion, posing a risk of missed detections. This could result in misjudgments or errors in practical quantum information tasks, thereby adversely affecting the efficiency and accuracy of these tasks.

We aim to explore the potential risk of missing entangled states when applying the inseparability criterion to asymmetric two-mode squeezed states. To achieve this, we will compare the inseparability criterion with the PPT criterion, which is more reliable in detecting entanglement. The PPT criterion serves as a sufficient and necessary condition for two-mode squeezed states, determining the separability of a state by the positive definiteness of the partial transpose matrix of the two-mode Gaussian state. Specifically, the PPT criterion quantifies the entanglement properties by calculating the minimum symplectic eigenvalue of the covariance matrix,

Preprints.org (www.preprints.org) | NOT PEER-REVIEWED | Posted: 31 October 2024 doi:10.20944/preprints202410.2541.v1

$$Ent_{PPT} = \sqrt{\frac{\Gamma - \sqrt{\Gamma^2 - 4\det \boldsymbol{\sigma}}}{2}} < 1 \tag{6}$$

where $\Gamma = \det \boldsymbol{A} + \det \boldsymbol{B} - 2\det \boldsymbol{C}$. If the inequality holds, the two-mode Gaussian state is considered entangled, otherwise, it is separable. In Figure 2, we visually compare the inseparability and PPT criteria in defining the entanglement region under two scenarios: asymmetry in the intermodal correlation of orthogonal components and asymmetry in the entanglement modes. Specifically, Figure 2(a) shows the analysis of missed detections by the inseparability criterion in the case of asymmetry in the intermodal correlation orthogonal components, where we fix $n = m = 3$ and analyze the evolution of the criterion by varying the values of $\tilde{c}_1$ and $\tilde{c}_2$, with $\tilde{c}_i = c_i / c_{\max}$, where the state is maximally entangled when $\tilde{c}_i = 1$; Figure 2(b) illustrates the analysis of missed detections by the inseparability criterion in the case of asymmetry in the entanglement modes, where we fix $\tilde{c}_1 = -\tilde{c}_2 = 1/\sqrt{2}$ and vary the values of n and m. In each subfigure, the orange region represents the entanglement range defined by the inseparability criterion, while the blue region shows the more comprehensive and rigorous entanglement definition given by the PPT criterion. The green region, a non-physical region, is defined by the constraints of Equation (3), reflecting the range of quantum states that are unattainable in actual physical systems. From the figures, it is evident that compared to the PPT criterion, the inseparability criterion covers a smaller region, entirely contained within the blue region defined by the PPT criterion. This indicates that the inseparability criterion fails to identify some entangled states recognized by the PPT criterion, highlighting the presence of missed entanglement detections. More specifically, in the case of ideal symmetric states (diagonally distributed from top left to bottom right in Figure 2(a) and anti-diagonally distributed from top right to bottom left in Figure 2(b)), the boundaries of the two criteria coincide, indicating that their judgments are equivalent: the inseparability criterion is both a sufficient and necessary condition for two-mode squeezed states. However, when this symmetry is broken, whether due to asymmetry in the intermodal correlation orthogonal components or asymmetry inherent in the entanglement modes—a significant divergence between the boundaries of the two criteria emerges, which deepens as asymmetry increases. This phenomenon reveals that under such circumstances, the inseparability criterion serves only as a sufficient condition, rather than a necessary, condition for determining whether a two-mode Gaussian state possesses entanglement properties. Consequently, when dealing with two-mode squeezed states with significant asymmetry, it may be necessary to apply the inseparability criterion more cautiously or consider using a more robust and rigorous criterion (such as the PPT criterion) that is less sensitive to asymmetry to ensure accurate entanglement detection.

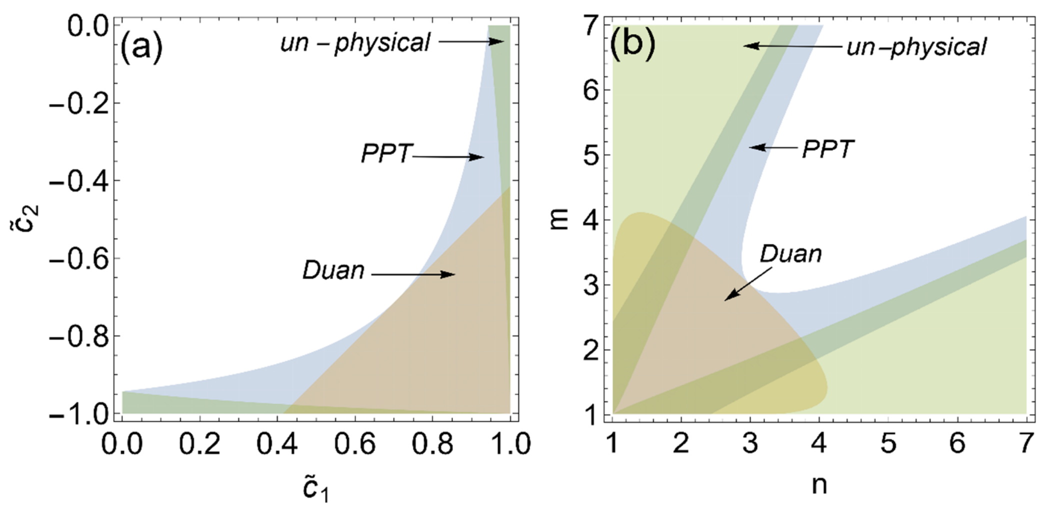

Figure 2. Contour plots illustrating the impact of entanglement asymmetry on entanglement criteria. (a) Asymmetry in correlated orthogonal components: With $n = m = 3$, the entanglement criterion is

Preprints.org (www.preprints.org) | NOT PEER-REVIEWED | Posted: 31 October 2024 doi:10.20944/preprints202410.2541.v1

shown as it evolves with respect to $\tilde{c}_1$ and $\tilde{c}_2$; (b) Asymmetry in entanglement modes: With $\tilde{c}_1 = -\tilde{c}_2 = 1/\sqrt{2}$, the evolution of the entanglement criterion is depicted with respect to n and m . The orange represents the entanglement region defined by the inseparability criterion, while the blue region delineates the entanglement range according to the PPT criterion. The green region indicates unphysical covariance matrices.

3. Experimental and Results

Our experimental validation was conducted through a NOPA system. Owing to the symmetry of the Hamiltonian, the state generated by NOPA is a fully symmetric state, implying that the elements of covariance matrix satisfy conditions, specifically $n = m$ and $c_1 = -c_2$. Figure 3 illustrates the experimental setup employed to generate the two-mode squeezed state. The NOPA comprises an α-cut type-II phase-matched KTiOPO4 (KTP) crystal (cut at 1°) and a plano-concave mirror. The system utilizes 1080 nm infrared light, noise-reduced by a three-mirror ring-cavity infrared mode cleaner (MC1), and 540 nm green light, noise-reduced by a green light mode cleaner (MC2), as the input and pump beams respectively. The NOPA cavity is operated below threshold, and when the relative phase between the pump and input beams is locked to the parametric deamplification state, the output port emits a two-mode squeezed state with orthogonal polarizations (signal field a and idler field b). This two-mode squeezed state exhibits anti-correlation in the quadrature amplitudes and positive correlation in the quadrature phases. In the experiment, the two sub-modes and of the two-mode squeezed state are separated using a polarizing beam splitter (PBS) and then directed to a balanced homodyne detection system for entanglement measurement. To achieve a lower pump threshold, the NOPA cavity is designed to be triply resonant for the pump, signal, and idler modes. This is experimentally realized by fine-tuning the phase-matching temperature and adjusting the transverse position of the crystal. During measurements, the system is operated at approximately 70% of the threshold power to avoid undesirable non-Gaussian effects. The experiment demonstrates a squeezing of -4.95 dB and an anti-squeezing of 6.53 dB at an analysis frequency of 2 MHz (see Figure 4). These measurements were obtained using a balanced homodyne detection system with a total detection efficiency of up to 85%. Complete measurements of the quadrature components allowed for the derivation of the covariance matrix, enabling a comparison between the PPT criterion and the inseparability criterion.

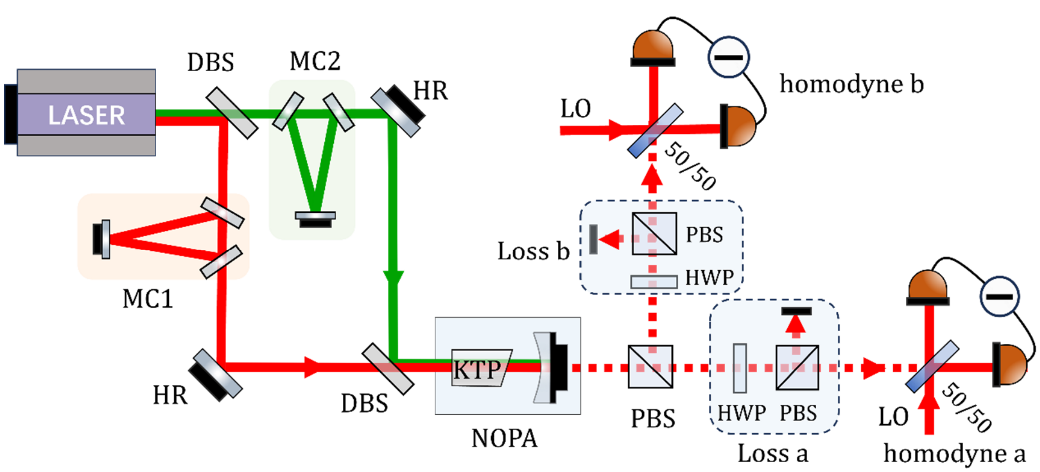

Figure 3. Schematic of the experiment. NOPA: non-degenerate optical parametric amplifier; MC1: mode cleaner; MC2: mode cleaner; HWP: half-wave plate; PBS: polarizing beamsplitter; DBS: dichroic beamsplitter.

 doi:10.20944/preprints202410.2541.v1

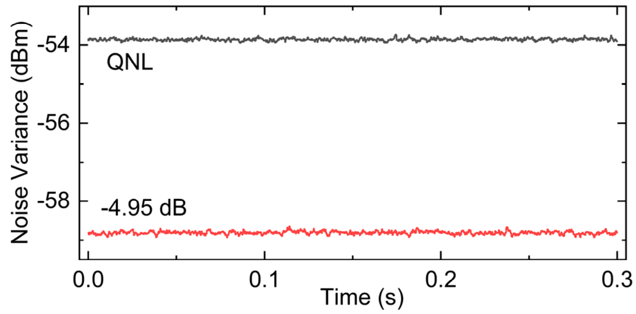

Figure 4. Measured entanglement spectrum at analysis frequency of 2MHz with inseparability criterion.

To introduce asymmetry in the entanglement, we strategically positioned independent beam splitters on the two entangled beams, prior to their arrival at the balanced homodyne detectors. This setup simulates propagation losses inherent quantum channels. These beam splitters were constructed using a half-wave plate and a polarizing beam splitter, enabling us to simulate channel attenuation ranging from 0% to 100% by adjusting the angle of the half-wave plate. The fields a' and b' preceding the balanced homodyne detectors can be mathematically expressed as $a' = \sqrt{\eta_a}a + \sqrt{1-\eta_a}a_v$ and $b' = \sqrt{\eta_b}b + \sqrt{1-\eta_b}b_v$, where $\sqrt{\eta_a}$ and $\sqrt{\eta_b}$ represent the channel transmission, and a_v and b_v are the vacuum fields introduced into the system due to the lossy channels. The two-mode Gaussian state $\rho_{a'b'}$, formed by the fields a' and b', can be effectively characterized by a covariance matrix:

$$\boldsymbol{\sigma}' = \begin{bmatrix} \eta_a n + 1 - \eta_A & 0 & \sqrt{\eta_a \eta_b}c & 0 \\ 0 & \eta_a n + 1 - \eta_a & 0 & -\sqrt{\eta_a \eta_b}c \\ \sqrt{\eta_a \eta_b}c & 0 & \eta_b n + 1 - \eta_b & 0 \\ 0 & -\sqrt{\eta_a \eta_b}c & 0 & \eta_b n + 1 - \eta_b \end{bmatrix} \tag{7}$$

For each attenuation, the inseparability value and PPT value are obtained by repeating the complete measurement process of the quadrature components. These entanglement criteria can be further formulated as functions of the channel attenuation, with the inseparability value,

$$\begin{aligned} Ent'_{Inse} &= \Delta^2 X^{+}_{a'\pm b'} + \Delta^2 X^{-}_{a'\pm b'} \\ &= \frac{1}{2}\left(\eta_a n + \eta_b n + (1-\eta_a) + (1-\eta_b) + 2\sqrt{\eta_a \eta_b}c\right) \end{aligned} \tag{8}$$

and PPT value,

$$Ent'_{PPT} = \sqrt{\frac{\Gamma' - \sqrt{\Gamma'^2 - 4\det \boldsymbol{\sigma}'}}{2}} \tag{9}$$

$$\Gamma' = \left(\eta_a n + 1 - \eta_a\right)^2 + \left(\eta_b n + 1 - \eta_b\right)^2 + 2\eta_a \eta_b c^2 \tag{10}$$

$$\det \boldsymbol{\sigma}' = \left[\left(\eta_a n + 1 - \eta_a\right)\left(\eta_b n + 1 - \eta_b\right) - \eta_a \eta_b c^2\right]^2 \tag{11}$$

Figure 5 presents the experimental outcomes for entanglement detection utilizing the inseparability criterion. Panels (a) and (b) illustrate the scenarios of symmetric ($\eta_a = \eta_b = \eta$) and asymmetric channel attenuation ($\eta_a = 1$ and $\eta_b = \eta$), respectively. Value 1 represent the standard

Preprints.org (www.preprints.org) | NOT PEER-REVIEWED | Posted: 31 October 2024 doi:10.20944/preprints202410.2541.v1

quantum noise limit (QNL), acquired by blocking the entangled light and allowing only the local light to enter the balanced homodyne detection system. The red dots and blue squares correspond to experimental measurements based on the inseparability and PPT criterion, respectively, with their respective theoretical fits depicted by matching colored curves. Data was collected at 10 distinct channel attenuation points, spaced at 0.1 intervals. At zero channel attenuation, the initial entanglement degree was -4.95 dB, accompanied by an anti-squeezing of 6.34 dB, indicative of a state purity of 0.73. In the case of symmetric losses, the results from both criterions coincide, revealing al linear decrease in entanglement with the increasing losses, remaining below 1 within a certain range of channel attenuation $[0,1)$. Conversely, under asymmetric losses, as the asymmetry intensifies, the inseparability criterion diverges from the PPT criterion. Notably, when the asymmetry exceeds 0.83, the inseparability value surpasses 1, signifying its inability to detect the entangled state. This underscores the intricacies of asymmetric losses in entanglement detection and emphasizes the significance of selecting an appropriate criterion. The close alignment between experimental measurements and theoretical predictions validates both the accuracy of our theoretical analysis and the reliability of the experimental procedure.

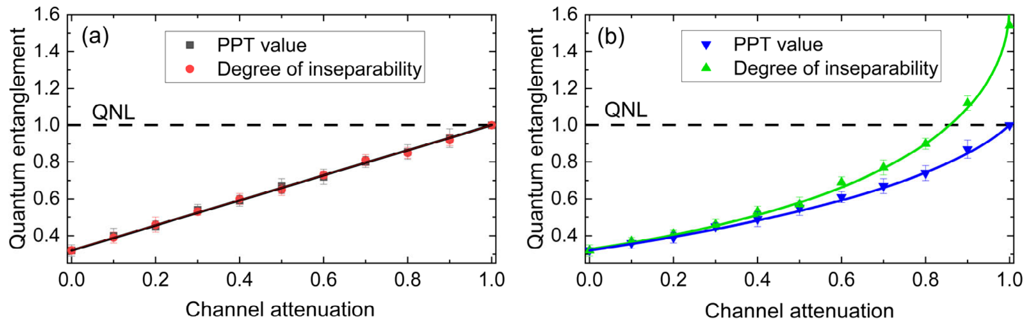

Figure 5. Experimental results of entanglement decoherence in lossy channel. (a) symmetric lossy channel; (b) asymmetric lossy channel.

In practical experimental setups, the presence of cavity losses and noise effects inherent to optical oscillators necessitates the preparation and manipulation of mixed states rather than pure states. Consequently, these states fail to uphold the minimum uncertainty principle, i.e., $\Delta^2 X_a^+ \bullet \Delta^2 X_a^- = \Delta^2 X_b^+ \bullet \Delta^2 X_b^- > 1$, yielding a purity metric that falls short of the ideal unity value. To delve into the implications of input state purity on entanglement assessment criteria, we conducted an analysis as illustrated in Figure 6. By systematically varying the purity levels to 1.0, 0.40, 0.138, and 0.04, achieved by maintaining a constant squeezing parameter with $r_1 = 0.69$ and adjusting the anti-squeezing parameter to 0.69, 1.15, 1.7, and 2.3, respectively, we examined their influence. Figures (a) and (b) explicitly depict the effects of purity on entanglement criteria under symmetric and asymmetric loss conditions, respectively. Intriguingly, under symmetric losses, the inseparability criterion and the PPT criterion remain invariant to changes in the purity of the two-mode squeezed state, once the initial squeezing factor is established. Conversely, in the presence of asymmetric losses, the PPT criterion remains relatively immune, whereas the inseparability criterion becomes acutely sensitive to state purity. As purity diminishes, the violation of the inseparability criterion intensifies markedly, attributed to the heightened total uncertainty that may hinder the fulfillment of its criteria, ultimately hindering entanglement detection. Furthermore, an overemphasis on squeezing a single quadrature component can potentially lead to erroneous entanglement assessments.

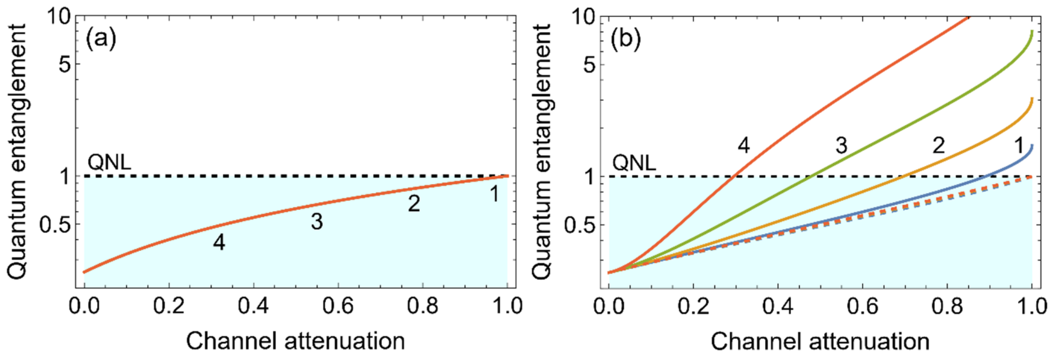

Figure 6. Effect of channel attenuation on the inseparability criterion for mixed entanglement state: (a) symmetric lossy channel; (b) asymmetric lossy channel.

4. Conclusions

This paper delves into the utilization of the inseparability criterion in assessing two-mode squeezed states, with a particular focus on analyzing the phenomenon of entanglement detection failures caused by entanglement asymmetry. To this end, we conducted a comparative analysis with the more stringent necessary and sufficient condition—PPT criterion, both theoretically and experimentally, investigating the instances where the inseparability criterion fails to detect entanglement. Experimentally, we employed a sub-threshold NOPA to generate two-mode squeezed states and introduced optical losses induce asymmetry in the entangled modes, thereby validating limitations of the inseparability criterion. Our results reveal that in the presence of symmetric entanglement, the inseparability criterion aligns with the PPT criterion, constituting a necessary and sufficient condition for two-mode Gaussian states. However, under asymmetry entanglement conditions, significant disparities emerge between the two criteria, with the inseparability criterion only serving as a sufficient condition. Consequently, exclusive reliance on the inseparability criterion may result in entanglement missed detection and erroneous entanglement assessments, with the misjudgment rate escalating alongside the intensification of entanglement asymmetry. Hence, when confronted with pronouncedly asymmetric two-mode squeezed states, a more prudent application of the inseparability criterion is warranted. This may involve adjusting the covariance matrix weights, incorporating compensation factors into the inseparability criterion calculation, or adopting stricter criteria to ensure accurate entanglement state determination. Additionally, exploring novel neural network-based methods for continuous-variable entanglement detection [42] offers promising avenues.

In conclusion, this study offers vital insights into the application and underlying principles of the inseparability criterion in quantum information tasks, while also highlighting its potential limitations. Future quantum information science research should prioritize the impact of asymmetric entanglement, continually refining entanglement detection and measurement methodologies. With ongoing research endeavors and technological advancements, we anticipate harnessing the extraordinary potential of quantum entanglement to propel the rapid evolution of quantum technologies.

Funding: Project supported by the National Natural Science Foundation of China (Grant No. 62005211，62071376，62001374，12304402，12004276), Sustainedly Supported Foundation by National Key Laboratory of Science and Technology on Space Microwave under Grant HTKJ2024KL504002, Key Research and Development Program of Shaanxi(2023KXJ-267), National Key Laboratory Foundation of China (2023-JCJQ-LB-007), Natural Science Foundation of Chongqing (No. CSTB2022NSCQ-BHX0700), Scientific and Technological Research Program of Chongqing Municipal Education Commission (No. KJQN202201217).

References

1. Huang, J., Li, X., Chen, X. *et al.*,: Demonstration of hypergraph-state quantum information processing. *Nat Commun* **15**, 2601 (2024). https://doi.org/10.1038/s41467-024-46830-7

2. Blais, A., Girvin, S.M. & Oliver, W.D.: Quantum information processing and quantum optics with circuit quantum electrodynamics. *Nat. Phys.* **16**, 247–256 (2020). https://doi.org/10.1038/s41567-020-0806-z
3. Li, W., Zhang, L., Tan, H. *et al.*: High-rate quantum key distribution exceeding 110 Mb s^{-1}. *Nat. Photon.* **17**, 416–421 (2023). https://doi.org/10.1038/s41566-023-01166-4
4. Chen, YA., Zhang, Q., Chen, TY. *et al.*,: An integrated space-to-ground quantum communication network over 4,600 kilometres. *Nature* **589**, 214–219 (2021). https://doi.org/10.1038/s41586-020-03093-8
5. Zapatero, V., van Leent, T., Arnon-Friedman, R. *et al.*: Advances in device-independent quantum key distribution. *npj Quantum Inf* **9**, 10 (2023). https://doi.org/10.1038/s41534-023-00684-x
6. Maring, N., Fyrillas, A., Pont, M. *et al.*,: A versatile single-photon-based quantum computing platform. *Nat. Photon.* **18**, 603–609 (2024). https://doi.org/10.1038/s41566-024-01403-4
7. Zhang Z S, You C, Magaña-Loaiza O S *et al.*,: Entanglement-based quantum information technology: a tutorial. *Advances in Optics and Photonics*, ***16*(1)**, 60-162. (2024). https://doi.org/10.1364/AOP.497143
8. Barbosa, F., Coelho, A., de Faria, A. *et al.*,: Robustness of bipartite Gaussian entangled beams propagating in lossy channels. *Nature Photon* **4**, 858–861 (2010). https://doi.org/10.1038/nphoton.2010.222
9. C. W. Sandbo Chang, A. M. Vadiraj, J. Bourassa, B. Balaji, C. M. Wilson: Quantum-enhanced noise radar. *Appl. Phys. Lett.* **114 (11)**: 112601 (2019). https://doi.org/10.1063/1.5085002
10. Karsa, Athena, Ghalaii Masoud and Pirandola Stefano.: Noiseless linear amplification in quantum target detection using Gaussian states. *Quantum Sci. Technol.* **7** 035026 (2022). https://doi.org/10.1088/2058-9565/ac781b
11. Gonzalez-Raya, T., Pirandola, S. & Sanz, M.: Satellite-based entanglement distribution and quantum teleportation with continuous variables. *Commun Phys* **7**, 126 (2024). https://doi.org/10.1038/s42005-024-01612-x
12. N. Hosseinidehaj, Z. *et al.*,: Satellite-Based Continuous-Variable Quantum Communications: State-of-the-Art and a Predictive Outlook. *IEEE Commun. Surv. Tutor.* **21** 881-919 (2019). https://doi.org/10.1109/COMST.2018.2864557
13. Steinlechner S, Bauchrowitz J, Eberle T, Schnabel R: Strong Einstein-Podolsky-Rosen steering with unconditional entangled states. *Phys. Rev. A* **87** 022104 (2013). https://doi.org/10.1103/PhysRevA.87.022104
14. Reid M D, Drummond P D.: Quantum correlations of phase in nondegenerate parametric oscillation. *Phys Rev Lett.* **60(26)**:2731-2733 (1988). https://doi.org/10.1103/PhysRevLett.60.2731
15. Simon R: Peres-Horodecki separability criterion for continuous variable systems. *Phys. Rev. Lett.* **84** 2726 (2000). https://doi.org/10.1103/PhysRevLett.84.2726
16. Tserkis S, Ralph T C: Quantifying entanglement in two-mode Gaussian states. *Phys. Rev. A* **96** 062338 (2017). https://doi.org/10.1103/PhysRevA.96.062338
17. Duan L M, Giedke G, Cirac J I, Zoller P: Inseparability Criterion for Continuous Variable Systems. *Phys. Rev. Lett.* **84** 2722 (2000). https://doi.org/10.1103/PhysRevLett.84.2722
18. Fedrizzi, A., Ursin, R., Herbst, T. *et al.*,: High-fidelity transmission of entanglement over a high-loss free-space channel. *Nature Phys* **5**, 389–392 (2009). https://doi.org/10.1038/nphys1255
19. Xu, JS., Xu, XY., Li, CF. *et al.*,: Experimental investigation of classical and quantum correlations under decoherence. *Nat Commun* **1**, 7 (2010). https://doi.org/10.1038/ncomms1005
20. Deng, X., Liu, Y., Wang, M. *et al.*,: Sudden death and revival of Gaussian Einstein–Podolsky–Rosen steering in noisy channels. *npj Quantum Inf* **7**, 65 (2021). https://doi.org/10.1038/s41534-021-00399-x
21. Li F, Li T, Agarwal G S: Experimental study of decoherence of the two-mode squeezed vacuum state via second harmonic generation. *Phys. Rev. Res.* **3** 033095 (2021). https://doi.org/10.1103/PhysRevResearch.3.033095
22. Buono D, Nocerino G, Porzio A, Solimeno S: Experimental analysis of decoherence in continuous-variable bipartite systems. *Phys. Rev. A* **86** 042308 (2012). https://doi.org/10.1103/PhysRevA.86.042308

23. Bowen W P, Schnabel R, Lam P K, Ralph T C: Experimental investigation of continuous-variable quantum teleportation, *Phys. Rev. Lett.* **90** 043601 (2003). https://doi.org/10.1103/PhysRevA.67.032302
24. Chunxiao Cai, Long Ma *et al.,* : Generation of a continuous-variable quadripartite cluster state multiplexed in the spatial domain. *Photon. Res.* **6** 479-484 (2018) https://doi.org/10.1364/PRJ.6.000479
25. Juan Li, Jiaming Li, Chunxiao Cai *et al.*,: Enhancement of continuous-variable hyperentanglement by optimizing pump mode. *Acta Phys. Sin.* **68** 034204 (2019). https://doi.org/10.7498/aps.68.20181625
26. G. Masada: Evaluation Method for Inseparability of Two-Mode Squeezed Vacuum States in a Lossy Optical Medium. *Tamagawa University Quantum ICT Research Institute Bulletin*, **5(1)** 19-23 (2015).
27. Masada G: Two-mode squeezed light source for quantum illuminaiton and quantum imaging II, *Proc. SPIE 9980 Quantum Commun. Quantum Imaging XIV* 99800T (2016).
28. Masada G: Verification of quantum entanglement of two-mode squeezed light source towards quantum radar and imaging. *Proc. SPIE 10409 Quantum Commun. Quantum Imaging XV* 104090P (2017).
29. Masada G: Non-Classical Correlation of Asymmetric Two-Mode Squeezed Vacuum states. *Tamagawa University Quantum ICT Research Institute Bulletin* **7** 33 (2017).
30. Masada G: Non-classical correlation of two-mode squeezed light in asymmetric optical-loss conditions. *Proc. SPIE 10771 Quantum Commun. Quantum Imaging XVI* 107710I (2018).
31. Jinxia Feng, Zhenju Wan *et al.*,: Distribution of continuous variable quantum entanglement at a telecommunication wavelength over 20 km of optical fiber. *Opt. Lett.* **42** 3399-3402 (2017). https://doi.org/10.1364/OL.42.003399
32. Hao Zhao, Jinxia Feng *et al.*,: Entanglement robustness of continuous variable Einstein-Podolsky-Rosen-entangled state distributed over optical fiber channel. *Acta Phys. Sin.* **71** (2022). https://doi.org/10.7498/aps.71.20212380
33. Wenhui Zhang, Ruixin Li *et al.*,: Security analysis of continuous variable quantum key distribution based on entangled states with biased correlations. *Opt. Express* **29** 22623-22635 (2021). https://doi.org/10.1364/OE.426089
34. David Luong, Bhashyam Balaji: Quantum two-mode squeezing radar and noise radar: covariance matrices for signal processing. *IET Radar Sonar Navig.* **14** 97 (2020). https://doi.org/10.1049/iet-rsn.2019.0090
35. Quntao Zhuang: Quantum Ranging with Gaussian Entanglement. *Phys. Rev. Lett.* **126** 240501 (2021). https://doi.org/10.1103/PhysRevLett.126.240501
36. Cyril Branciard, Eric G. Cavalcanti *et al.*,: One-sided device-independent quantum key distribution: Security, feasibility, and the connection with steering. *Phys. Rev. A* **85** 010301 (2012). https://doi.org/10.1103/PhysRevA.85.010301
37. Katherine Wagner, Jiri Janousek *et al.*,: Asymmetric EPR entanglement in continuous variable systems. *J. Phys. At. Mol. Opt. Phys.* **47** 225502 (2014). https://doi.org/10.1088/0953-4075/47/22/225502
38. Bowen, W. P., Lam, P. K., & Ralph, T. C.: Biased EPR entanglement and its application to teleportation. 2003 *J. Mod. Opt.* **50** 801–813 (2003). https://doi.org/10.1080/09500340308235187
39. Zhao J: Post-selection-based continuous variable quantum information processing. PhD thesis Australian National University 2019.
40. M. Houde, L.C.G. Govia, and A.A. Clerk: Loss Asymmetries in Quantum Traveling-Wave Parametric Amplifiers. *Phys. Rev. Applied* **12** 034054 (2019). https://doi.org/10.1103/PhysRevApplied.12.034054

doi:10.20944/preprints202410.2541.v1

41. Spyros Tserkis, Jayne Thompson *et al.*,: Maximum entanglement of formation for a two-mode Gaussian state over passive operations. *Phys. Rev. A* **102** 052418 (2020). https://doi.org/10.1103/PhysRevA.102.052418
42. Xiaoting Gao, Mathieu Isoard *et al.:* Correlation-Pattern-Based Continuous Variable Entanglement Detection through Neural Networks. *Phys. Rev. Lett* **132** 220202 (2024). https://doi.org/10.1103/PhysRevLett.132.220202